FDTD Analysis of Resistor-Loaded Bow-Tie Antennas Covered with Ferrite-Coated Conducting Cavity for Subsurface Radar

Yasuhiro Nishioka, *Student Member, IEEE*, Osamu Maeshima, Toru Uno, *Member, IEEE*, and Saburo Adachi, *Life Fellow, IEEE*

***Abstract*—This paper presents a full-wave analysis of a ground penetrating radar (GPR) using the finite-difference time-domain (FDTD) method. The antenna treated here consists of a resistor-loaded bow-tie antenna, which is covered with a rectangular conducting cavity of which inner walls are coated partially or fully with ferrite absorber. Some techniques are introduced into the FDTD analysis to obtain the accurate results and to save the computer resources. The validity of the FDTD analysis is confirmed experimentally. Furthermore, the effects of the ferrite absorber on the GPR characteristics are theoretically investigated in detail. The FDTD results indicate that the remarkable improvement of the antenna characteristics for the GPR system cannot be attained by the ferrite absorber.**

***Index Terms*—Buried object detection, cavity-backed antennas, dipole antennas.**

I. Introduction

THE ground penetrating radar (GPR) or the subsurface radar is greatly expected as an effective tool for nondestructively sensing subsurface environment [1], [2]. Various GPR systems have been investigated and developed for detecting and identifying underground objects such as water pipes, power and communication lines, archaeological remains, and so on [1], [2]. However, conventional GPR systems are still insufficient for practical uses with respect to reliability, resolution, detectable depth, and so forth. In order to overcome these difficulties, it is important to improve characteristics of signals to be measured as well as signal processing and imaging methods for detecting the underground objects. Therefore, the design and development of antennas of higher performances would be invaluable.

The purpose of this paper is to theoretically investigate the characteristics of the GPR antenna by using the finite-difference time-domain (FDTD) method. Some calculated results are compared with experiments to confirm the validity of the theory. The antenna considered here is most often used bow-tie antenna. The antenna is covered with a conducting cavity to prevent electromagnetic radiation from affecting other electric systems and also to prevent the antenna from receiving the undesired signal arrived from the air. The bow-tie antenna is connected to the cavity through lumped resistors. The loaded resistor is considered to damp the natural oscillation of the antenna and to contrast the signal scattered by the underground target.

Bourgeois and Smith [3] have analyzed a similar GPR system described here by using FDTD method. Their results are essentially valid only for the scattering in early time because they used the perfect conductor wall on the outer surface of computation space. The wall reflections were removed by the time windowing and the subtraction procedure. However, these approaches are not always possible because the multiple scatterings such as wall–wall reflections and antenna-interface interaction are very complicated. Therefore, some important properties such as the antenna impedance and the late-time scattering by the object cannot be calculated. Furthermore, it is considered from a computational point of view that the FDTD method should be improved because the geometry of the bow-tie antenna does not fit in with the rectangular cells. Thus, the accurate computation of the GPR system including the scattering by the underground object is still uncompleted. In addition, in most practical GPR's, a wave absorber is attached to the inner walls of the conducting cavity to reduce the multiple reflection in the cavity. A ferrite sheet is often used for the wave absorber with an expectation that it will improve the GPR antenna because the ferrite has a good absorption property over VHF/UHF frequency range. However, the ferrite is a extremely weighty material. Therefore, in order to secure the transportability with maintaining the good property, it is necessary to optimize the volume and position of the ferrite.

In this paper, a fully three-dimensional FDTD method is applied to analyze the resistor-loaded bow-tie antenna, which is covered with the rectangular metallic cavity of which inner walls are coated partially or fully with the frequency-dependent ferrite absorber. In all calculations presented in this paper, Berenger's perfectly matched layer (PML) absorbing boundary condition [10] is used. In Section II, some FDTD implementations to analyze the GPR antenna are described.

Manuscript received July 21, 1998; revised March 1, 1999.

Y. Nishioka and T. Uno are with the Department of Electrical and Electronic Engineering, Tokyo University of Agriculture and Technology, Koganei-shi, 184-8588 Japan.

O. Maeshima is with the KDD R&D Laboratories, Kamifukuoka-shi, 356-8502 Japan.

S. Adachi is with the Department of Communication Engineering, Tohoku Institute of Technology, Sendai-shi, 982-8577 Japan.

Publisher Item Identifier S 0018-926X(99)05803-2.

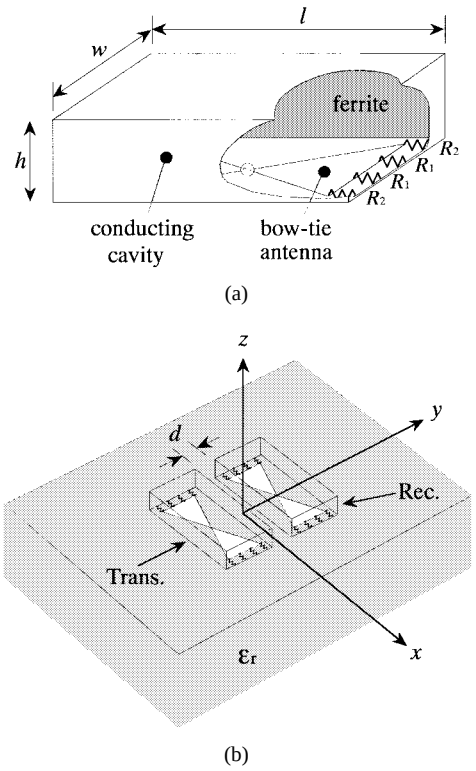

Fig. 1. (a) Geometry of GPR antenna. (b) Two GPR antennas above the ground surface and coordinate system.

First, an accurate modeling of the bow-tie antenna based on the contour-path method is implemented in the FDTD update equations. Next, the FDTD computation technique using a surface impedance boundary condition (SIBC) for the frequency-dependent ferrite sheet backed by a perfect conductor used in this GPR is described briefly. Third, an equivalent circuit model for analyzing the transmitting and receiving characteristics of a bistatic GPR are presented. The FDTD results, including these techniques, are compared with experiments in order to confirm the validity of the analysis. In Section III, the input impedance and near-field radiation pattern of the GPR located above the ground surface are calculated. The transient receiving voltages scattered by an underground object are also calculated. All the possible characteristics are thoroughly discussed for contrasting the effects of the ferrite absorber.

II. Some Techniques for Analyzing GPR and Experimental Confirmation

Fig. 1(a) shows the geometry of the GPR antenna considered in this paper. The bow-tie antenna is covered with the rectangular conducting cavity and its each edge is connected to the cavity through four lumped resistors. The inner walls of the cavity are coated with ferrite sheets fully or partially. The same GPR antennas are placed above a ground surface and parallel each other as shown in Fig. 1(b). One of which is a transmitting antenna and other a receiving antenna.

Thus, the GPR antenna treated here is very complicated, so some relevant techniques are required for analyzing the antenna. In this section, we will implement several FDTD computation techniques sequentially. The validity of the computations is in part confirmed experimentally.

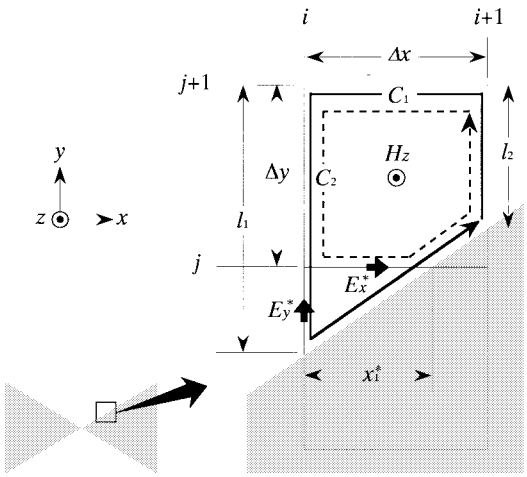

Fig. 2. FDTD cells near the slanted edge of the bow-tie antenna.

A. Modeling of Bow-Tie Antenna

The original FDTD method approximates a smoothly curved or slanted surface by staircase boundaries. The error caused by the staircase approximation is not so small for antenna impedance and near fields. The subcell methods [16]–[18], which locally modify the algorithms for the field components of the particular cells in the vicinity of the interface, are useful for accurately modeling arbitrarily shaped objects. The basic idea of the subcell algorithm described here is similar to the contour path (CP) method described in [17], [18], but the resultant update equations are somewhat different from the original CP method because the arrangement of the contour path is modified in this paper. Therefore, we will describe here the subcell method specialized to the bow-tie antenna briefly.

Let the face of a bow-tie antenna be placed on the $z = k\Delta z$ plane as shown in Fig. 2. The update equations for all of the field components near the slanted edge, except for the z-component electric field, should be modified. For the configuration shown in Fig. 2, the modified components correspond to E_x^* and E_y^*. In the original CP method, the E_x^* and E_y^* are replaced by $E_x(i-1/2, j, k)$ and $E_y(i, j+1/2, k)$, respectively. This is referred to as "nearest neighbor approximation." However, the nearest neighbor approximation should be modified to calculate the bow-tie antenna characteristics more accurately, because the electromagnetic fields near the conducting edge is quite complex. In this paper, we modified the calculation of E_x^* and E_y^* as follows.

The z-component magnetic field H_z can be supposed constant on the all surfaces bounded by the closed contour C_1 (solid line) or C_2 (broken line). Applying Faraday's law to both contours, the following equation can be obtained:

$$\frac{1}{S_1}\int_{C_1}\mathbf{E}\cdot d\mathbf{l} = \frac{1}{S_2}\int_{C_2}\mathbf{E}\cdot d\mathbf{l} \tag{1}$$

where S_1 and S_2 are the area of the cell surface bounded by the C_1 and C_2, respectively. Transforming (1) to the FDTD

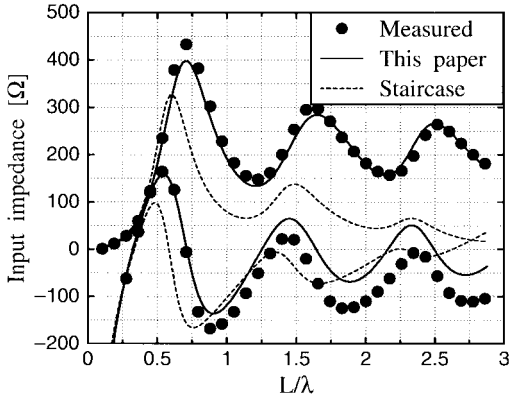

Fig. 3. Comparison of the input impedances of a bow-tie antenna calculated by our subcell method and the staircase approximation.

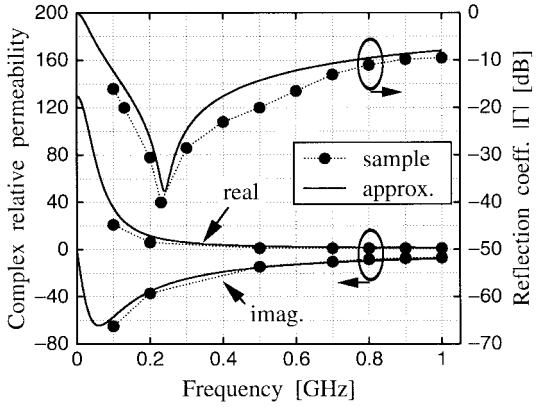

Fig. 4. Frequency characteristics of the complex relative permeability and reflection coefficient of the commercially provided ferrite sheet.

form, the update equation for the E_x^* is given by

$$E_x^{*n}(i^*,j,k) = \frac{\Delta x(1-\alpha)}{x_1^*}E_x^n\left(i+\frac{1}{2},j+1,k\right) - \frac{l_2^*(1-\alpha)}{x_1^*}E_y^n\left(i+1,j+\frac{1}{2},k\right) + \frac{\Delta y(1-\alpha)}{x_1^*}E_y^n\left(i,j+\frac{1}{2},k\right) + \frac{\alpha h_2}{x_1^*}E_y^{*n}(i+1,j^*,k) - \frac{\alpha h_1}{x_1^*}E_y^{*n}(i,j^*,k) \tag{2}$$

where

$$l_2^* = \begin{cases} l_2; & l_2 \le \Delta y \\ \Delta y; & l_2 \ge \Delta y \end{cases} \tag{3}$$

$h_1 = l_1 - \Delta y$, $h_2 = l_2 - l_2^*$, and $\alpha = S_2/S_1$. Thus, in our method, the E_x^* is calculated from the electric field components at the same time-step. $E_y^*(i,j^*,k)$ is extrapolated by $E_y(i,j{+}1/2,k)$ and $E_y(i,j{+}3/2,k)$. The update equations for the H-field components can be easily derived by using the original CP method [17], [18].

Fig. 3 shows the frequency characteristics of the input impedance of a bow-tie antenna calculated by using this method or the staircase approximation. The total length of the antenna is L and its flare angle is 45°. In this calculation, the size of a cubical Yee cell was $L/21$ and the time step was chosen as the Courant limit. The result obtained from this modeling agree well with the measured data over a wide frequency range as compared to the staircase approximation. Thus, the remarkable improvement can be achieved by using this subcell method.

B. Treatment of Ferrite Sheet Backed by PEC

The ferrite sheet considered here is commercially provided one whose thickness is 6 mm. All of the constitutive parameters of the ferrite sheet are not published, but the measured complex permeability and reflection coefficient are given at discrete frequencies. In this paper, first the required constitutive parameters were assumed as

$$\epsilon = \epsilon_0\epsilon_r + \frac{\sigma}{j\omega}, \tag{4}$$

$$\mu = \mu_0\left(\mu_\infty + \frac{\mu_s - \mu_\infty}{1+j\omega\tau_0}\right). \tag{5}$$

Next, the unknown parameters included in the above equations were determined by using curve fitting method. The estimated parameters resulted in $\mu_s = 130$, $\mu_\infty = 1$, $\tau_0 = 1/(12\pi{\times}10^7)$ sec, $\epsilon_r = 28$, and $\sigma = 0.001$ S/m. The frequency characteristics of the permeability and reflection coefficient of the ferrite sheet are shown in Fig. 4. The approximated curves agree relatively well with the published data.

The wavelength in the ferrite is much shorter than that of free-space because the ferrite has high constitutive parameters described above. This requires much finer cells and large computer resources for accurately computing the fields within the ferrite. However, if the external fields are only of interest, a surface impedance boundary condition (SIBC) can be effectively applied to the interface. This eliminates the need to use much finer cells throughout the whole FDTD computation space. Several SIBC's for lossy materials having constant constitutive parameters have been proposed [4]–[8]. However, these SIBC's cannot be applied directly to the ferrite backed by a conductor discussed here because the strong dispersion is caused by both material dispersion itself and multiple reflection in the sheet. The SIBC for a lossy dielectric layer backed by a perfect electric conductor (PEC) has been studied [9], however, the layer was assumed to be physically very thin and the multiple reflection within the layer was neglected. On the other hand, the authors have implemented the SIBC for a dispersive layer backed by a PEC taking account of multiple reflection [20], [21]. This SIBC can be applied directly to analyze the scattering due to the ferrite-coated conducting cavity. Therefore, only the basic idea will be shown here.

When $|\epsilon\mu/\epsilon_0\mu_0| \gg 1$ as for the ferrite, the surface impedance is independent both of a polarization and an incident angle of an incident field and is approximated by

$$Z_s(s) = \sum_{l=1}^{L} \frac{2d\mu s}{d^2\epsilon\mu s^2 + P_l^2} \tag{6}$$

where $P_l = (2l-1)(\pi/2)$, $s = j\omega$, L is the truncated number of the series expression of a tangential function and d is the thickness of the sheet. The transient electric field on the ferrite

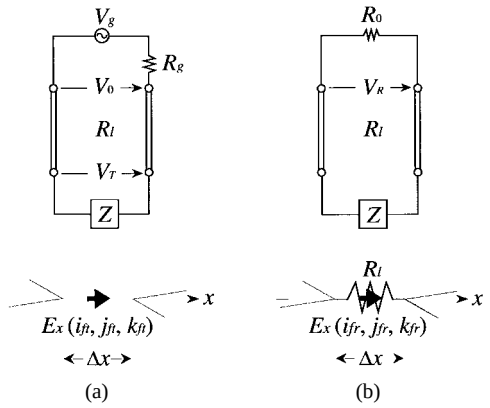

Fig. 5. Equivalent circuits of (a) the transmitting system and (b) the receiving system.

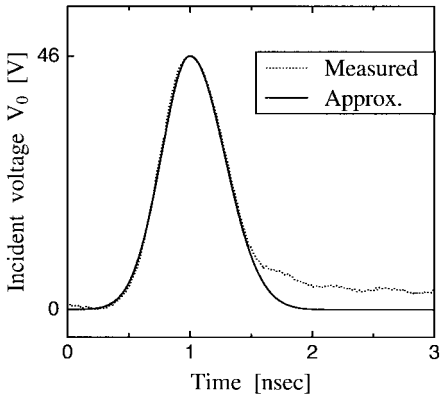

Fig. 6. Incident pulse.

surface is expressed by a convolution integral of the magnetic field and the corresponding time-domain surface impedance

$$Z_s(\tau) = \sum_{l=1}^{L} \sum_{p=1}^{3} c_{l,p} e^{s_{l,p}\tau} \tag{7}$$

where $s_{l,p}$ $(p = 1, 2, 3)$ are three poles of (6) which are all single order for the parameters described above and $c_{l,p}$ are the residue for each pole. The convolution integral can be evaluated recursively for the surface impedance expressed by the sum of exponential functions such as (7). In this paper, the piecewise linear recursive convolution (PLRC) method described in [19] was used for evaluating the convolution integral.

C. Equivalent Circuit Model

In this section, let us discuss how the antenna is fed and how the receiving signal is calculated in the FDTD framework. While extremely accurate results can be obtained if the feed region is modeled precisely, the whole FDTD space should be restricted because of the limited computer memory. In [3], a parallel-wire transmission line was modeled into FDTD computation. However, the conductors of the transmission lines may not affect the surrounding fields considerably because the transmission line or a coaxial cable is usually arranged perpendicularly to the antenna conductor. The time delay of the signal between both ends of the cable can be easily estimated. Therefore, there is no particular problem if the transmission line or the coaxial cable is modeled by an equivalent circuit. In this paper, the equivalent circuit model is incorporated into the FDTD calculation. Using this model, any special cell modifications are not needed.

Fig. 5(a) shows the equivalent circuit of the transmitting system and the feed point of the transmitting antenna. V_g is the source voltage, Z_g is the internal impedance of the signal generator, and Z is the input impedance of the antenna. Assuming that the transmission line is lossless and neglecting the multiple reflection and time delay between the ends of the transmission line, the voltage at the terminal V_T is expressed as $V_T = 2V_0 - R_l I$, where V_0 is the incident voltage, R_l is the characteristic resistance of the transmission line, and I is the electric current. The electric field component at the terminal of the transmitting antenna is then given by

$$E_x^n(i_{ft}, j_{ft}, k_{ft}) = -\frac{2V_0^n - R_l I^{n-\frac{1}{2}}}{\Delta x}. \tag{8}$$

The current I is calculated from the magnetic field components surrounding the $E_x(i_{ft}, j_{ft}, k_{ft})$. The $1/2$ time-step offset between the current and the voltage is caused from the $1/2$ time-step offset between the electric and magnetic fields representation in FDTD method.

The equivalent circuit of the receiving system and the terminal port of the receiving antenna are shown in Fig. 5(b). R_0 is the internal resistance of the receiver. The transient received voltage at the receiver V_R is given by

$$V_R^n = -\Delta x E_x^n(i_{fr}, j_{fr}, k_{fr}) \frac{2R_0}{R_0 + R_l}. \tag{9}$$

In the above equations, the values of R_l and R_0 can be chosen arbitrarily in the computational point of view, but a reasonable choice for R_l is to use the value of the characteristic resistance of the transmission line or coaxial cable. We chose $R_0 = R_l = 50\ \Omega$ in all of the following calculations.

D. Comparison with Experiment

In order to confirm the validity of the methods described in the previous sections, FDTD results are compared with experimental results. The sizes of the bow-tie antenna and the cavity, the values of the loaded resistors, and other parameters are as follows [see Fig. 1(a)]. The total length of the bow-tie antenna is 24.6 cm and its flare angle is 67.4°. The cavity size is $l = 31$ cm, $w = 21$ cm, and $h = 11$ cm. The upper face and two side faces of the inner walls are coated with the ferrite sheet described in Section II-B. The resistors whose values are $R_1 = \infty$ and $R_2 = 200\ \Omega$ are connected between the bottom of the cavity and the edge of the bow-tie antenna. The two same GPR antennas, one of which is the transmitting antenna and the other the receiving antenna are placed in free-space [$\epsilon_r = 1$ in Fig. 1(b)] and parallel to each other. The distance between them is $d = 3.6$ cm.

The incident voltage V_0 is shown in Fig. 6. The dotted line shows the measured voltage generated from a pulse generator. The solid line shows the approximated Gaussian pulse, which is used for the FDTD calculation. In our calculation, we used

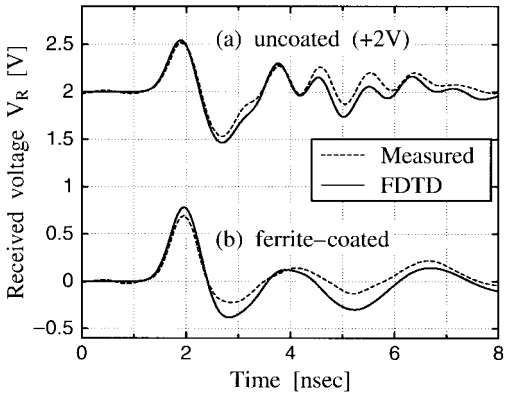

Fig. 7. Comparison of the received voltages obtained from the FDTD method and the experiment. The transmitting and receiving antennas are located in free-space. (a) The results for the uncoated. (b) The results for the ferrite coated.

the cubical cell whose size is 0.6 cm and the time step was chosen as Courant limit.

The FDTD and experimental results of the received voltage are shown in Fig. 7, where the uncoated data is illustrated by shifting the actual data by two voltages. In both cases, the agreement is excellent, but there is a slight difference between them. This difference might be caused mainly by the error of the approximation for the incident pulse. Thus, the effectiveness of the FDTD calculation and the validity of the methods described above have been confirmed experimentally.

It is noted here that the dispersion property of a resistor should be involved to obtain more accurate results, because some practical resistors show frequency dependency, particularly in a high-frequency range. This dispersion characteristics will be easily incorporated into FDTD update equations using the PLRC method, for example. However, in the above calculation, the resistors have been assumed to be independent of frequency because the measurement of the dispersion of the resistor is quite difficult in high-frequency range.

III. The Effects of Ferrite Absorber on GPR Characteristics

In this section, the characteristics of the GPR located above the ground surface are calculated to investigate the effects of the ferrite absorber. In the FDTD calculation, the cell size, time step, and incident pulse are the same as those in Section II.D, but the GPR antenna treated here is slightly different from the one treated in Section II.D. The size of the cavity are $l = 29.4$ cm, $w = 20.4$ cm, and $h = 6$ cm. The values of the resistors are $R_1 = 330\ \Omega$ and $R_2 = 470\ \Omega$. The height of the antennas is 0.6 cm. The relative permittivity of the ground is $\epsilon_r = 4$.

Actual soil consists of frequency-dependent, inhomogeneous, lossy materials. Although the conventional absorbing boundary conditions (ABC's) based on the one-way wave equation are able to be applied to the dispersive medium, their accuracy is not so high because the velocity in the dispersive medium depends on frequency and cannot be determined uniquely. On the other hand, the original Berenger's PML-ABC has been extended to the one for dispersive media [22]. Therefore, actual soil might be simulated in a FDTD analysis if

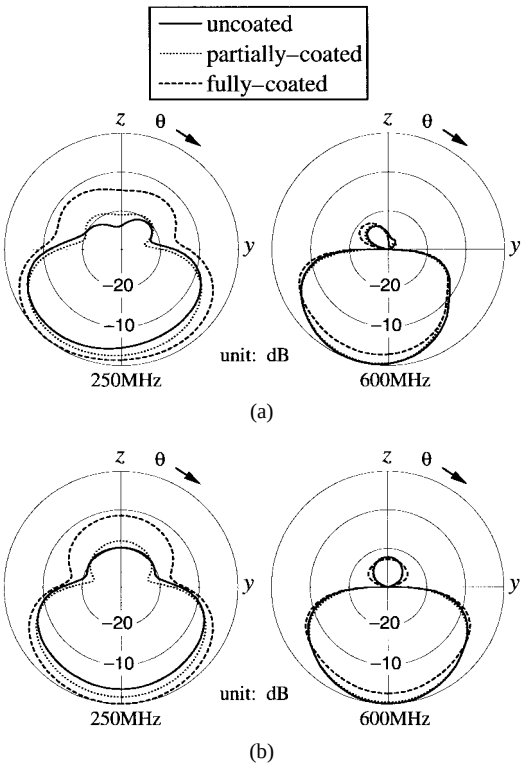

Fig. 8. Near-field pattern of E_x in the y-z plane at the frequencies of 250 MHz and 600 MHz. (a) Two antennas. (b) Single antenna.

the electrical properties of the soil including the dispersivility and inhomogeneity are known completely. However, the soil property greatly depends upon the circumstances such as water content and constitutive particles. Therefore, even if complicated properties of soil are taken into consideration, the obtained results may not have generality, except for specific applications. Furthermore, it is considered that the loss, dispersivility, and inhomogeneity of soil may not affect considerably to the ferrite effect on the antenna characteristics of the GPR. For the above reasons, the ground is assumed to be an uniform lossless nondispersive dielectric half-space in this paper.

A. Near-Field Pattern

The origin of the coordinate system is located on the ground surface and at the center of the antennas. The radial distance between the origin and the observation points is set to $r = 60$ cm.

Fig. 8(a) shows the near-filed patterns of main polarization E_x at the frequencies of 250 MHz and 600 MHz. The "partially coated" denotes the result when the ferrite is attached to only the upper face of the cavity, and "fully coated" denotes the one when the inner surfaces are fully coated with the ferrite. In the fully coated case, the undesired radiation to the air is large as compared to the other two cases, especially at 250 MHz. Fig. 8(b) shows the pattern of the single antenna at the same frequencies. The similar conclusions to the above two antennas case are observed. Therefore, the enhancement of the undesired radiation is not caused by a mutual coupling of the antenna, but by ferrite coating.

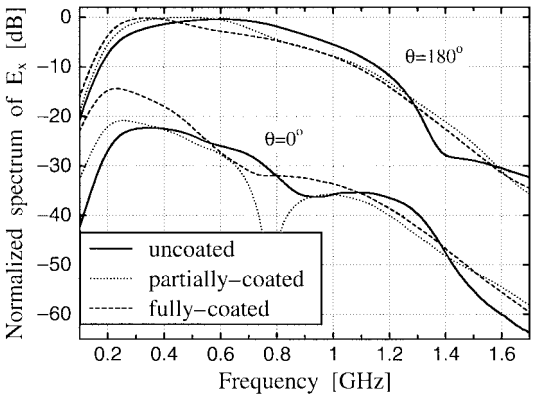

Fig. 9. Spectrum of E_x at the angles of $\theta = 0°$ and $\theta = 180°$.

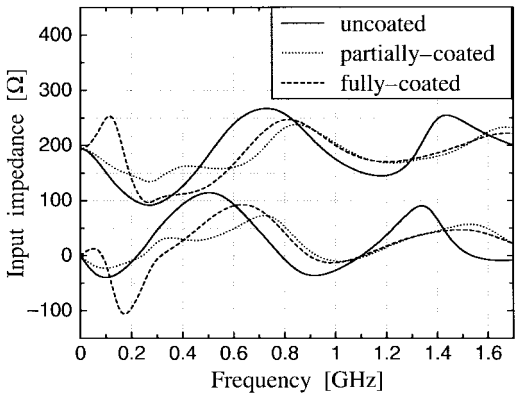

Fig. 10. Input impedance versus frequency.

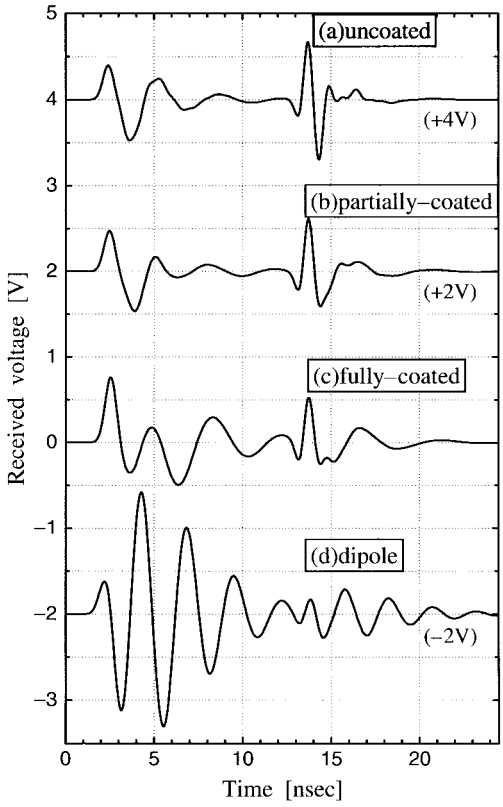

Fig. 11. Comparison of the received voltages.

Fig. 9 shows the frequency characteristics of E_x just above ($\theta = 0°$) and just below ($\theta = 180°$) the antennas. At $\theta = 180°$, the three cases make relatively little difference in the level over the wide-frequency range. On the other hand, at $\theta = 0°$, the magnitude of E_x increases in the lower frequency range when the inner surfaces of the cavity are fully coated with the ferrite sheets.

From Figs. 8 and 9, it is found that while the desired radiation to the underground is the same level in all cases, the undesired radiation to the air is enhanced by the ferrite, particularly in the low-frequency range. This is considered that the electric current flowing on the outer surfaces of the cavity increased by attaching the ferrite to the inner surfaces. These results indicate that "shielding effect" due to the conducting cavity is reduced by ferrite coating.

B. Input Impedance

The broad-band impedance characteristic is required for the GPR antenna over a wide-frequency range in order to radiate an electromagnetic pulse with little distortion. Fig. 10 shows frequency characteristics of the input impedance of the GPR antenna for the three cases. It is found that the broad-bandness is attained by coating with the ferrite partially or fully on the whole, but remarkable improvement cannot be attained over the wide-frequency range. However, the partially coated case shows its effectiveness for a relatively low-frequency range. On the other hand, for the fully-coated case the impedance characteristic in a lower frequency range (approximately up to 200 MHz) is inferior to the other two cases. This indicates that a mono-pulse including a large quantity of low-frequency spectrum, as shown in Fig. 6, will be distorted considerably when it is radiated from the antenna. It is noted here that for this type of GPR antenna the undesired radiation to the air is possibly increased when the impedance matching characteristic is improved by attaching the wave absorber to the inner walls of the cavity.

C. Receiving Characteristic

Fig. 11 shows the transient received voltage when a very thin 29.4-cm × 30-cm rectangular PEC sheet is buried just below the center of the transmitting and receiving antennas at the depth of 90 cm. The early time signals are the contributions from the direct coupling between two antennas and from the reflection at the ground surface. The peaks at approximately 14 ns are the signal scattered by the buried PEC.

When the inner walls of the cavity are fully coated with the ferrite sheets, a ringing of the signal increases for a long period. This ringing is considered to be caused by the direct coupling, not by the natural resonance of the antenna itself because that the radiated field in the air is enlarged in the fully coated case as discussed in the previous section. Moreover, the distortion of the target signal is more severer than the other two cases. This distortion is due to the poor impedance characteristic in the lower frequency range, as shown in Fig. 10.

It is also found from Figs. 10 and 11 that the amplitudes of the target signals are all the same order even if the broad-band

impedance characteristic was attained by ferrite coating. This is due to the fact that the radiation to the air is enhanced by attaching the ferrite as mentioned in Section III-A.

The received voltage for two bare dipole antennas with the length of 30.6 cm is also shown in Fig. 11(d) for comparison. The directly coupled signal and antenna ringing are serious as compared to the bow-tie case and it is impossible to distinguish the target signal only from this waveform.

IV. Conclusion

The resistor-loaded bow-tie antenna which is covered with the ferrite-coated cavity has been analyzed by using FDTD method. In the first half of this paper, some techniques for analyzing the GPR have been implemented. The input impedance of a bow-tie antenna and the receiving characteristic of the bistatic GPR located in free-space were calculated and measured in order to confirm the validity of these techniques. The results were in good agreement and demonstrated the validity of our methods.

In the second half, the effects of the ferrite on the GPR characteristics were investigated in detail for the optimization of the GPR antenna. It was found that the impedance characteristic of the GPR antenna was improved some extent by attaching the ferrite sheets to the inner walls of the cavity partially or fully. However, for the type of GPR antenna discussed in this paper, the undesired electromagnetic wave radiated to the air was enhanced by attaching the ferrite especially to the whole inner walls of the cavity. This is considered that the electric current flowing on the outer faces of the cavity increased by coating the inner faces with the ferrite. This result indicates that "shielding effect" due to the conducting cavity decreases by ferrite coating. It was also found that the ringing in the received signal which is mainly due to the direct coupling between the transmitting and receiving antennas, was enhanced by attaching the ferrite. Furthermore, the target signal scattered by the buried object was distorted by ferrite-coating. Thus, there is no remarkable advantages obtained by coating the inner surfaces of the cavity with the ferrite absorber at least for the structures investigated in this paper. An investigation for other type of GPR's will be next important theme.

Acknowledgment

The authors would like to thank Dr. Y. He for his comments on the FDTD calculation of the bow-tie antenna. They would also like to thank E&C Engineering K.K. for supplying the measured data of the characteristics of the ferrite sheet.

References

[1] L. Peters Jr., J. J. Daniels, and J. D. Young, "Ground penetrating radar as a subsurface environmental sensing tool," *Proc. IEEE*, vol. 82, pp. 1802–1822, Dec. 1994.
[2] D. J. Daniels, D. J. Gunton, and H. F. Scott, "Introduction to subsurface radar," *Proc. Inst. Elect. Eng.*, vol. 135, pt. F, pp. 278–320, Aug. 1988.
[3] J. M. Bourgeois and G. S. Smith, "A fully three-dimensional simulation of a ground-penetrating radar: FDTD theory compared with experiment," *IEEE Trans. Geosci. Remote Sensing*, vol. 34, pp. 36–44, Jan. 1996.
[4] J. G. Maloney and G. S. Smith, "The use of surface impedance concepts in the finite-difference time-domain method," *IEEE Trans. Antennas Propagat.*, vol. 40, pp. 38–48, Jan. 1992.
[5] J. H. Beggs, R. J. Luebbers, K. S. Yee, and K. S. Kunz, "Finite-difference time-domain implementation of surface impedance boundary conditions," *IEEE Trans. Antennas Propagat.*, vol. 40, pp. 49–56, Jan. 1992.
[6] K. S. Yee, K. Shlager, and A. H. Chang, "An algorithm to implement a surface impedance boundary condition for FDTD," *IEEE Trans. Antennas Propagat.*, vol. 40, pp. 833–837, July 1992.
[7] T. Kashiwa, O. Chiba, and I. Fukai, "A formulation for surface impedance boundary conditions using the finite-difference time-domain method," *Microwave Opt. Tech. Lett.*, vol. 5, no. 10, pp. 486–490, 1992.
[8] S. Kellali, B. Jecko, and A. Reineix, "Implementation of a surface impedance formalism at oblique incidence in FDTD method," *IEEE Trans. Electromagn. Compat.*, vol. 35, pp. 347–356, Aug. 1993.
[9] J. H. Beggs, "A FDTD surface impedance boundary condition using Z-transforms," *Appl. Computat. Electromagn. Soc. J.*, vol. 13, no. 1, pp. 14–24, Mar. 1998.
[10] J.-P. Berenger, "A perfectly matched layer for the absorption of electromagnetic waves," *J. Computat. Phys.*, vol. 114, pp. 185–200, Oct. 1994.
[11] J. G. Maloney, G. S. Smith, and W. R. Scott Jr., "Accurate computation of the radiation from simple antenna using the finite-difference time-domain method," *IEEE Trans. Antennas Propagat.*, vol. 38, pp. 1059–1068, July 1990.
[12] K. L. Shlager, G. S. Smith, and J. G. Maloney, "Optimization of bow-tie antennas for pulse radiation," *IEEE Trans. Antennas Propagat.*, vol. 42, pp. 975–982, July 1994.
[13] K. S. Yee, "Numerical solution of initial boundary value problems involving Maxwell's equations in isotropic media," *IEEE Trans. Antennas Propagat.*, vol. AP-14, pp. 302–307, May 1966.
[14] R. J. Luebbers and K. Kunz, "Finite difference time domain calculation of antenna mutual coupling," *IEEE Trans. Antennas Propagat.*, vol. 39, pp. 1203–1212, Aug. 1991.
[15] R. J. Luebbers, L. Chen, T. Uno, and S. Adachi, "FDTD calculation of radiation patterns, impedance, and gain for a monopole antenna on a conducting box," *IEEE Trans. Antennas Propagat.*, vol. 40, pp. 1577–1583, Dec. 1992.
[16] J. G. Maloney and G. S. Smith, "The efficient modeling of thin material sheets in the finite-difference time-domain (FDTD) method," *IEEE Trans. Antennas Propagat.*, vol. 40, pp. 323–330, Mar. 1992.
[17] T. G. Jurgens, A. Taflove, K. Umashankar, and T. G. Moore, "Finite-difference time-domain modeling of curved surface," *IEEE Trans. Antennas Propagat.*, vol. 40, pp. 357–366, Apr. 1992.
[18] T. G. Jurgens and A. Taflove, "Three-dimensional contour FDTD modeling of scattering from single and multiple bodies," *IEEE Trans. Antennas Propagat.*, vol. 41, pp. 1703–1708, Dec. 1993.
[19] D. F. Kelly and R. J. Luebbers, "Piecewise linear recursive convolution for dispersive media using FDTD," *IEEE Trans. Antennas Propagat.*, vol. 44, pp. 792–797, June 1996.
[20] T. Uno, *FDTD Method for Electromagnetic and Antenna Analyzes*. Tokyo, Japan: Corona, Mar. 1998, sec. 10.5, pp. 254–259.
[21] Y. Nishioka, O. Maeshima, T. Uno, and S. Adachi, "FDTD implementation of surface impedance boundary condition for dispersive layer backed by perfect conductor," *IEICE Trans. Electron.*, vol. E81-C, no. 12, pp. 1902–1904, Dec. 1998.
[22] T. Uno, Y. He, and S. Adachi, "Perfectly matched layer absorbing boundary condition for dispersive medium," *IEEE Microwave Guided Wave Lett.*, vol. 7, pp. 264–266, July 1997.

Yasuhiro Nishioka (S'98) was born in Tokyo, Japan, on July 2, 1971. He received the B.S. and M.S. degrees in electrical and electronic engineering from Tokyo University of Agriculture and Technology, Japan, in 1995 and 1997, respectively. He is currently working toward the Ph.D. degree in the Department of Electrical and Electronic Engineering at the same university.

His research interests are antennas and imaging method for subsurface radar.

Osamu Maeshima received the B.E. and M.E. degrees from Tohoku University, Sendai Japan, in 1992 and 1994, respectively.

In 1994, he joined KDD Corporation, Tokyo, Japan, where he was engaged in network service operation. Since 1996 he has been at KDD R&D Laboratories Inc. and is currently engaged in research on computer networks and telecommunications.

Mr. Maeshima is a member of the Institute of Electronics, Information, and Communication Engineers (IEICE).

Toru Uno (M'86) received the B.S. degree in electrical engineering from Tokyo University of Agriculture and Technology, Tokyo, Japan, in 1980, and the M.S. and Ph.D. degrees in electrical engineering from Tohoku University, Sendai, Japan, in 1982 and 1985, respectively.

In 1985, he was appointed as a Research Associate in the Department of Electrical Engineering of Tohoku University. From 1991 through 1994 he was an Associate Professor of the same university. He is presently a Professor in the Department of Electrical and Electronics Engineering of Tokyo University of Agriculture and Technology (TUAT). From 1998 through 1999 he was on leave from the TUAT to join the Electrical Engineering Department at the Pennsylvania State University, University Park, PA, as a Visiting Scholar. His research interests include electromagnetic inverse problem, computational electromagnetics, medical and subsurface radar imagings, and electromagnetic compatibility.

Dr. Uno received the Young Scientist Award from the Institute of Electronics, Information and Communication Engineers (IEICE) in 1990. He is a member of IEICE, AGU, ACES, Japan Society for Simulation Technology, and Japan Society of Archaeological Prospection.

Saburo Adachi (S'57–M'59–SM'62–F'84–LF'95) was born in Yamagata Prefecture, Japan, on September 2, 1930. He received the B.S., M.S., and Ph.D. degrees in electrical communication engineering, all from Tohoku University, Sendai, in 1953, 1955, and 1958, respectively.

In 1958, he was appointed as Research Associate in the Department of Electrical Communication Engineering, Tohoku University. From 1958 to 1960 he was on leave from Tohoku University to join the Antenna Laboratory, The Ohio State University, Columbus, OH, as a Research Associate (also as Fullbright Scholar). He was an Associate Professor at Tohoku University from 1961 and a Professor from 1970 to 1994. He is presently a Professor of Tohoku Institute of Technology, Sendai. He has been engaged in research on large loop antennas including the invention of one-wavelength directive loop antenna, conical antennas, geodesic Luneburg lens antennas, birefringent circular polarizer, antennas in plasmas, radiation and propagation of electromagnetic and electrostatic waves in plasmas, antennas for fusion plasma heating, superconducting small antennas, array antenna theory, and antenna measuring distance. He has also studied on various electromagnetic wave theories such as electromagnetic wave backscattering from slender conducting bodies of an arbitrary shape (originator of extended physical optics current method), radar target imaging, and multiple backscattering from random media, medium-frequency broadcasting antennas on elevated ground, etc. His current research includes radio wave power transmission, inverse scattering problems, antennas for mobile communications, penetration and shielding of electromagnetic wave in human bodies, antennas for MRI, numerical analysis of 3-D scattering problems using FDTD method, underground radar imaging, and various electromagnetic environmental problems.

Dr. Adachi is an honorary member of IEICE and a member of the Engineering Academy of Japan and the Electromagnetics Academy.